END

DTIC

MICROCOPY RESOLUTION TEST CHART

NATIONAL BUREAU OF STANDARDS-1963-A

Increased Hot-Electron Production at Quarter-Critical Density in Long-Scalelength, Laser-Plasma Interactions

F. C. YOUNG, M. J. HERBST,* C. K. MANKA*
S. P. OBENSCHAIN,* AND J. H. GARDNER†

Plasma Technology Branch
Plasma Physics Division

Laser Plasma Branch
Plasma Physics Division

†*Laboratory for Computational Physics*

February 11, 1985

NAVAL RESEARCH LABORATORY
Washington, D.C.

85   02   05_018

REPORT DOCUMENTATION PAGE

1a. REPORT SECURITY CLASSIFICATION UNCLASSIFIED		1b. RESTRICTIVE MARKINGS		
2a. SECURITY CLASSIFICATION AUTHORITY		3. DISTRIBUTION / AVAILABILITY OF REPORT Approved for public release; distribution unlimited.		
2b. DECLASSIFICATION / DOWNGRADING SCHEDULE				
4. PERFORMING ORGANIZATION REPORT NUMBER(S) NRL Memorandum Report 5484		5. MONITORING ORGANIZATION REPORT NUMBER(S)		
6a. NAME OF PERFORMING ORGANIZATION Naval Research Laboratory	6b. OFFICE SYMBOL (If applicable) Code 4730	7a. NAME OF MONITORING ORGANIZATION		
6c. ADDRESS (City, State, and ZIP Code) Washington, DC 20375-5000		7b. ADDRESS (City, State, and ZIP Code)		
8a. NAME OF FUNDING / SPONSORING ORGANIZATION Department of Energy	8b. OFFICE SYMBOL (If applicable)	9. PROCUREMENT INSTRUMENT IDENTIFICATION NUMBER		
8c. ADDRESS (City, State, and ZIP Code) Washington, DC 20545		10. SOURCE OF FUNDING NUMBERS		

PROGRAM ELEMENT NO.	PROJECT DE- NO. AI08- 79DP40092	TASK NO.	WORK UNIT ACCESSION NO. DN220-133

11. TITLE (Include Security Classification) Increased Hot-Electron Production at Quarter-Critical Density in Long-Scalelength, Laser-Plasma Interactions

12. PERSONAL AUTHOR(S)
Young, F.C., Herbst, M.J., Manka, C.K., Obenschain, S.P., and Gardner, J.H.

13a. TYPE OF REPORT Interim	13b. TIME COVERED FROM 9/84 TO 10/84	14. DATE OF REPORT (Year, Month, Day) 1985 February 11	15. PAGE COUNT 15

17	COSATI CODES		18. SUBJECT TERMS (Continue on reverse if necessary and identify by block number)
FIELD	GROUP	SUB-GROUP	Laser-plasma interactions, Hot-electron temperature
			Long-scalelength plasma Plasma instabilities.

19. ABSTRACT (Continue on reverse if necessary and identify by block number)   Sq cm

Hot-electron fractions measured in Nd-laser-plasma interactions at 10^{14} W/cm² increase from <0.02% to 0.3% as the plasma scalelength at quarter-critical density ($n_c/4$) is systematically increased from 140 μm to 320 μm. Correlated x-ray and $3\omega/2$ emissions indicate that the hot electrons are produced by a $n_c/4$ instability. (originator-supplied keywords include.)

Accession For

NTIS GRA&I

DTIC TAB

Unannounced

20. DISTRIBUTION / AVAILABILITY OF ABSTRACT ☒ UNCLASSIFIED/UNLIMITED ☐ SAME AS RPT ☐ DTIC USERS	21. ABSTRACT SECURITY CLASSIFICATION UNCLASSIFIED	
22a. NAME OF RESPONSIBLE INDIVIDUAL F. C. Young	22b. TELEPHONE (Include Area Code) (202) 767-3066	22c. OFFICE SYMBOL Code 4770

DD FORM 1473, 84 MAR   83 APR edition may be used until exhausted
          All other editions are obsolete

Availability Codes

Dist Avail and/or Special

A-1

SECURITY CLASSIFICATION OF THIS PAGE

INCREASED HOT-ELECTRON PRODUCTION AT QUARTER-CRITICAL DENSITY
IN LONG-SCALELENGTH, LASER-PLASMA INTERACTIONS

Laser-plasma interactions in long-scalelength plasmas are of increasing importance to laser fusion as larger underdense plasmas are produced with more energetic lasers and larger targets.[1] The energy-coupling processes in the long-scalelength, underdense region of such targets may include plasma instabilities which have not been been important in previous experiments at shorter scalelength. For example, thresholds for the Raman[2] and two-plasmon-decay[3-5] ($2\omega_p$) instabilities are expected to decrease with increasing plasma scalelength. These instabilities are important for laser fusion even if they account for only a small fraction of the total absorption, because they generate hot electrons which preheat the target fuel and impede fuel compression.

The Raman and $2\omega_p$ instabilities have been observed in many laser-plasma experiments,[6] including some with longer plasma scalelengths ($L = n/|\nabla n| > 100\,\mu m$ at $n_c/4$). However, previous experiments have not included systematic variations of plasma scalelength. A technique for controlled scalelength variations has been reported previously and used in absorption-efficiency measurements.[7] In this paper, we report the first hot-electron measurements as a function of plasma scalelength, using this technique to systematically vary the plasma scalelength. Thresholds for energetic x-rays, indicative of hot-electron production, are observed with either increasing irradiance or scalelength. Measured correlations of energetic x-ray and $3\omega/2$ emissions (where ω is the laser frequency) identify hot-electron production with a nc/4 process, probably the $2\omega_p$ instability.

In the experiment, two Nd-laser beams ($\lambda = 1.054\ \mu m$) are used to give both long scalelength and high irradiance. A 4-nsec pulse irradiates planar polystyrene targets (150 to 180 μm thick) to produce long-scalelength background

plasmas. A second pulse of 0.3-nsec duration is timed to the peak of this pulse and focused to a smaller area (50% of the energy within 90 μm) to produce vacuum irradiances of 10^{14} to 10^{15} W/cm^2 for incident energies (E) of 4 to 40 J. The irradiance may change in the plasma due to self-focusing; there is experimental evidence for self-focusing only for E > 14 J, but beam propagation calculations suggest self-focusing at lower energies.[8] The background-plasma scalelength is changed by varying the focal size (0.36 to 1.08-mm diam) of the 4-nsec pulse while maintaining a constant irradiance of ~ 6×10^{12} W/cm^2. As described previously,[7] three different focal sizes correspond to short, medium and long scalelengths. At $n_c/4$, the measured axial scalelengths (L) are 140, 240, and 320 μm, respectively, in agreement with hydrodynamic calculations. At n_c, these calculations indicate that the axial scalelength is constant at 45 μm.

Temporally and spatially integrated x-ray spectra are used to evaluate hot-electron production and target heating. Detector arrays with K-edge filters[9] are used to measure x-ray intensities: seven PIN diodes for low photon energy (1 to 10 keV) and seven scintillator-photomultipliers for high photon energy (20 to 115 keV). No x rays with energies greater than 50 keV were detected in the experiment. Spectra are unfolded from measurements below 50 keV, and temperatures are extracted from spectral slopes. Emission below 10 keV is dominated by the 4-nsec laser pulse, which contains more energy than the short pulse. Temperatures from the 1 to 3 keV x-ray region are 280, 300, and 330 eV for short, medium, and long scalelengths, respectively. These temperatures are nearly equal because the irradiance of the 4-nsec pulse is approximately the same for each scalelength.

Energetic (> 20 keV) x-ray emission is dominated by the short, high-irradiance laser pulse. There is negligible contribution from the low-

irradiance, 4-nsec pulse. This emission is sensitive to the short-pulse energy
(E) and the preformed plasma scalelength (L). Measurements are made at 120° to
the incident-laser-beam direction, and isotropic emission into 4π sr is
assumed. For short L and low E, no energetic x rays are observed, as shown in
Fig. 1, but increasing either E or L causes an onset of energetic x rays (i.e.,
hot electrons). Hot-electron temperatures (T_h) range from 6 to 10 keV and have
little dependence on E. Also, only a weak dependence of T_h on L is observed.
The intensity of energetic x rays, defined as the integral above 20 keV of the
x-ray spectrum, is shown in Fig. 2 as a function of E for different L. At short
L, this intensity increases rapidly from an apparent threshold at $\approx$ 5 J
(corresponding to a vacuum irradiance of $\approx 1 \times 10^{14}$ W/cm^2). For longer L,
energetic x rays are detected even for laser energies less than 5 J, and their
intensity increases with L. For example, at 7 J a threshold is apparent between
short and medium scalelengths. This behaviour at low E contrasts with that at
higher E (20 J) where the x-ray intensity is nearly constant as L is increased.

The fraction of laser energy deposited in hot electrons is estimated from
the measured x-ray intensities and values of T_h. These fractions, which
correspond to the total energy in a Maxwellian distribution given by T_h, are
presented in Fig. 3 in terms of the scalelength at $n_c/4$. X-ray production by
thick-target bremsstrahlung with one-half of the electrons directed into the
target is assumed. For high energies (i.e., $\gtrsim$ 20 J), this fraction is not
sensitive to the change in scalelength at $n_c/4$. Many speculative explanations
may be offered for this observation, but at these higher energies the
perturbation of the background plasma by the short pulse[7] and the occurrence of
self-focusing[8] greatly complicate the interpretation. At lower energies (e.g.,
7 J), the increasing hot-electron fraction correlates with the scalelength
variation at $n_c/4$ and not with the nearly constant scalelength at n_c; this

suggests that the mechanism for hot-electron production at low energies is an underdense process.

To test for hot-electron production by $n_c/4$ instabilities, measurements correlating the intensities of $3\omega/2$ and energetic x-ray radiations are made at lower laser energies. The $3\omega/2$ light emitted in the plane of incidence at 30° and 45° with respect to the laser axis (24° and 39° relative to the target normal) is focused onto fiberoptic cables in the target chamber. These cables are coupled either to filtered photodiodes (350-psec risetime) or to a spectrograph and optical multichannel analyzer (OMA) to give time-integrated $3\omega/2$ spectra. The observed duration of this emission is detector-risetime limited, which indicates that the $3\omega/2$ light is due to the high-irradiance short pulse and not the 4-nsec pulse. Spectra from the OMA show the characteristic two-peaked distribution (centered near $3\omega/2$) that is usually attributed to processes involving the plasma waves of the $2\omega_p$ instability.[10]

The intensities of energetic x-ray and $3\omega/2$ emissions are correlated as the short-pulse energy (E) and plasma scalelength (L) are varied. Measurements obtained on the same laser shots are presented in Fig. 4. For short L, a detection threshold for energetic x rays is observed near 5 J; at this energy the $3\omega/2$ emission increases abruptly by more than an order of magnitude. Also, these radiations scale together with increasing E and L. This positive correlation implies hot-electron generation by a $n_c/4$ process because $3\omega/2$ emission is indicative of plasma density fluctuations near $n_c/4$.

Three processes that could drive plasma waves near $n_c/4$ (and the resultant hot electrons) are the convective Raman, the absolute Raman, and the $2\omega_p$ instabilities. Growth rates and thresholds are evaluated for these instabilities including Landau and collisional damping, as well as the effect of inhomogeneity. Convective Raman is unlikely in this experiment because its

4

theoretically-predicted growth rate[11] is the smallest; even for the longest scalelength, only one e-folding of growth is predicted at 10^{14} W/cm^2 (the irradiance at E = 5 J if there is no self-focusing). Thresholds (zero growth rate) for the absolute Raman instability[11] are about three times larger than values predicted for the $2\omega_p$ instability. Thus, the $2\omega_p$ instability is most likely responsible for hot electrons in this experiment. For a 600-eV plasma temperature at $n_c/4$ (based on hydrodynamic calculations at the peak of the short pulse), the predicted thresholds[3-5] are 4.6×10^{13} W/cm^2 and 2.6×10^{13} W/cm^2 for the short and long scalelengths, respectively. Calculated growth rates at 10^{14} W/cm^2 are 1.2×10^{12} sec^{-1}, and 1.8×10^{12} sec^{-1} which allow several e-foldings of growth in both cases. Furthermore, this instability most easily accounts for the two-peaked $3\omega/2$ spectra.

Measured values of T_h are significantly less than temperatures associated with electrons trapped in the most unstable plasma waves associated with these instabilities. For the conditions of this experiment, the most unstable waves have $k\lambda_d \lesssim 0.07$, where λ_d is the Debye length and k is the wave number. If T_h is given by the energy associated with the phase velocity of the most unstable waves,[12] then plasma-wave dispersion relations give $T_h = T_e[3 + (k\lambda_d)^{-2}]$ where T_e is the plasma thermal temperature. For T_e = 600 eV (at $n_c/4$) this expression implies $T_h \gtrsim 100$ keV. Measured values of T_h correspond to waves with $k\lambda_d \approx 0.25-0.4$, which are strongly Landau-damped and therefore less unstable. Perhaps the small measured T_h-values are explained by wave-energy cascading from the driven small-k modes to larger-k modes before coupling to the electrons; this process has been predicted theoretically[13] and has been observed in computer simulations of the $2\omega_p$ and Raman instabilities.[14]

As a final note, we contrast the results of this experiment with an earlier investigation in which the 0.3-nsec pulse was delayed by 5.4 nsec after the peak

of the 4-nsec pulse.[15] In this earlier experiment, no energetic x rays were observed from the short-pulse interaction with the plasma produced by the long pulse; the presence of the background plasma suppressed energetic x rays that were observed with the short pulse alone. This result was also obtained in experiments where a gas jet was used to preform a long-scalelength profile of cold neutral gas.[16] Obviously, conditions other than plasma scalelength (notably plasma temperature) can alter interactions in the underdense region. The present experiment with warmer preformed plasmas may more closely simulate conditions appropriate for high-gain laser fusion.

In conclusion, hot-electron production in laser-plasma interactions has been measured with controlled variations of the plasma scalelength. Correlations of energetic x rays with $3\omega/2$ emissions imply that hot electrons are produced by a $n_c/4$ process. Hot-electron production is enhanced at longer scalelength, as predicted by theory. However, hot-electron temperatures are substantially less than values based on the phase velocities of the most unstable waves for the $2\omega_p$ and Raman instabilities.

References

1. W.L. Kruer, Comments Plasma Phys. Cont. Fusion $\underline{6}$, 167 (1981).

2. C.S. Liu, M.N. Rosenbluth, and R.B. White, Phys. Fluids $\underline{17}$, 1211 (1974).

3. C.S. Liu and M.N. Rosenbluth, Phys. Fluids $\underline{19}$, 967 (1976).

4. B.F. Lasinski and A.B. Langdon, in Laser Program Annual Report, 1977, Vol. 2. edited by C.F. Bender and B.D. Jarman, Lawrence Livermore Laboratory, UCRL-50021-77, pp.4-49, 1978.

5. A. Simon, et al., Phys. Fluids $\underline{26}$, 3107 (1983).

6. See, for example, H. Figueroa, et al., Phys. Fluids $\underline{27}$, 1887 (1984), and references contained therein.

7. M.J. Herbst, et al., Phys. Rev. Lett. $\underline{52}$, 192 (1984).

8. J.A. Stamper, et al., U. S. Naval Research Laboratory Memorandum Report 5462, 1983; submitted to Phys. Fluids.

9. F.C. Young, in Laser-Fusion Studies at NRL, A Report to ERDA for July 1975 to Sept. 1976, edited by S.E. Bodner, Naval Research Laboratory Memorandum Report 3591, p.41, 1977, AD-A050089.

10. A.I. Avrov, et al., Sov. Phys. JETP $\underline{45}$, 507 (1977); P.D. Carter, S.M.L.Sim, and E.R. Wooding, Opt. Commun. $\underline{32}$, 443 (1980).

11. C.S. Liu, in Advances in Plasma Physics, edited by A. Simon and W.B. Thompson (Wiley, New York, 1976) Vol. 6, p. 121.

12. K. Estabrook, W.L. Kruer, and B.F. Lasinski, Phys. Rev. Lett. $\underline{45}$, 1399 (1980).

13. W.L. Kruer, Phys. Fluids $\underline{15}$, 2423,(1972).

14. A.B. Langdon, B.F. Lasinski, and W.L. Kruer, Phys. Rev. Lett. 43, 133 (1979); K. Estabrook and W.L. Kruer, Phys. Fluids 26, 1892 (1983).

15. M.J. Herbst, et al., Measurements of Laser Coupling and Plasma Profiles in Longer Scalelength Plasmas, Naval Research Laboratory Memorandum Report 4893, 1982, AD-A121043.

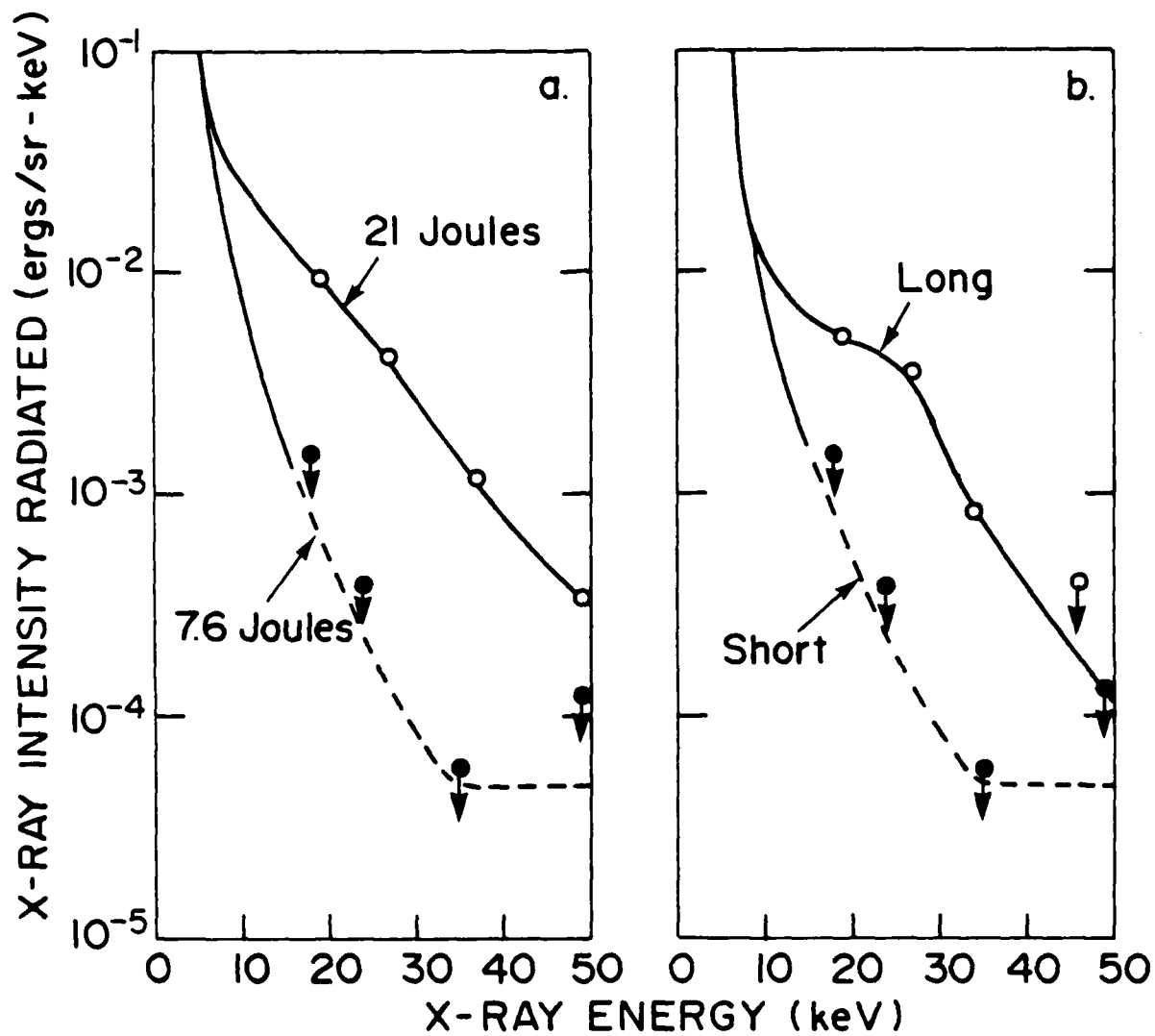16. J.A. Tarvin, et al., Phys. Rev. Lett. 48, 256 (1982).

Figure 1

Energetic x-ray spectra (a) at 7.6 J and 21 J laser energy for short
scalelength and (b) for short and long scalelengths at ≈ 7 J. Detection
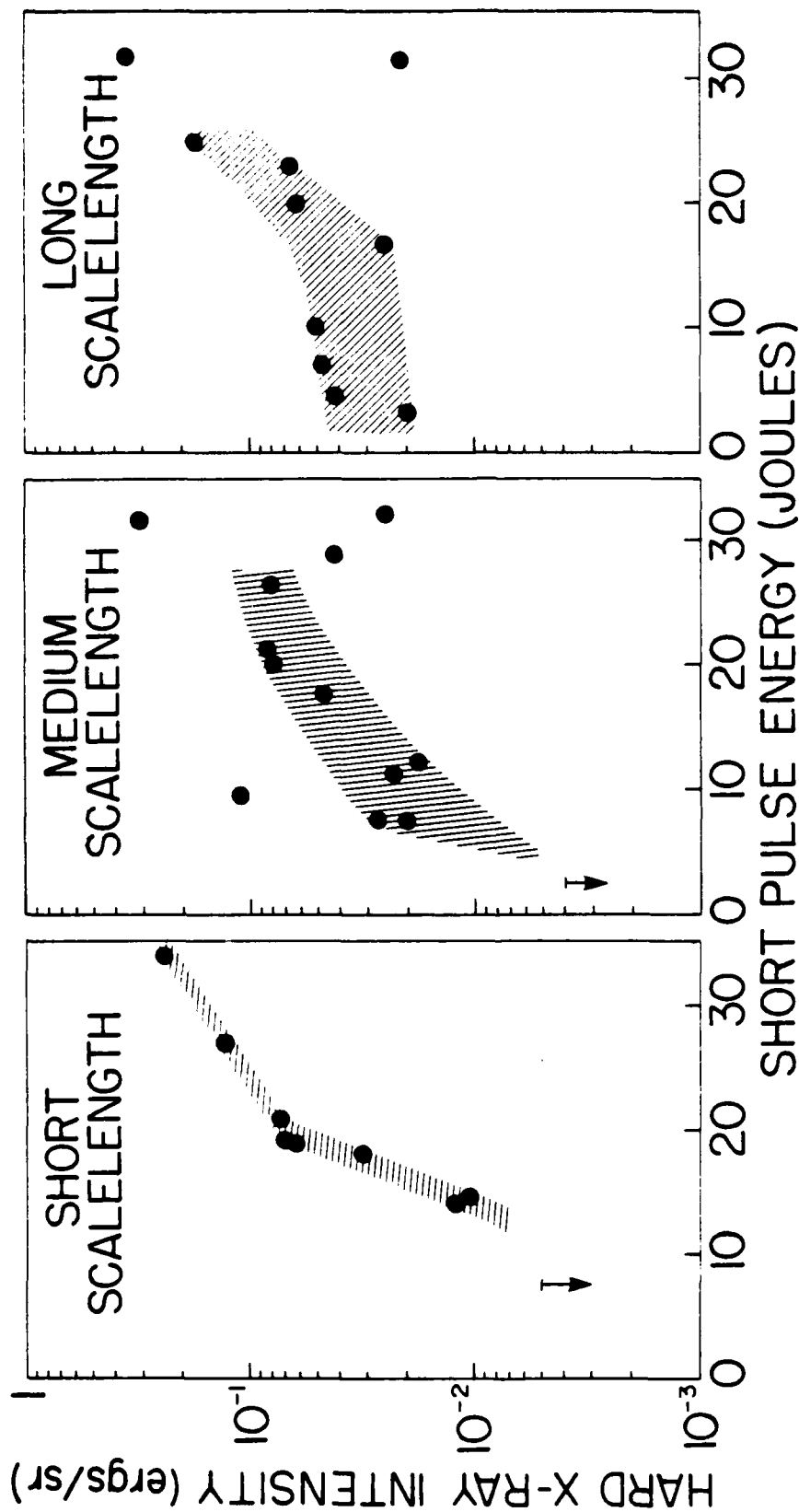limits are indicated by arrows.

9

Figure 2

Integrated x-ray intensities (20 to 50 keV) for different scalelength plasmas. Scatter in the data represents shot-to-shot reproducibility.
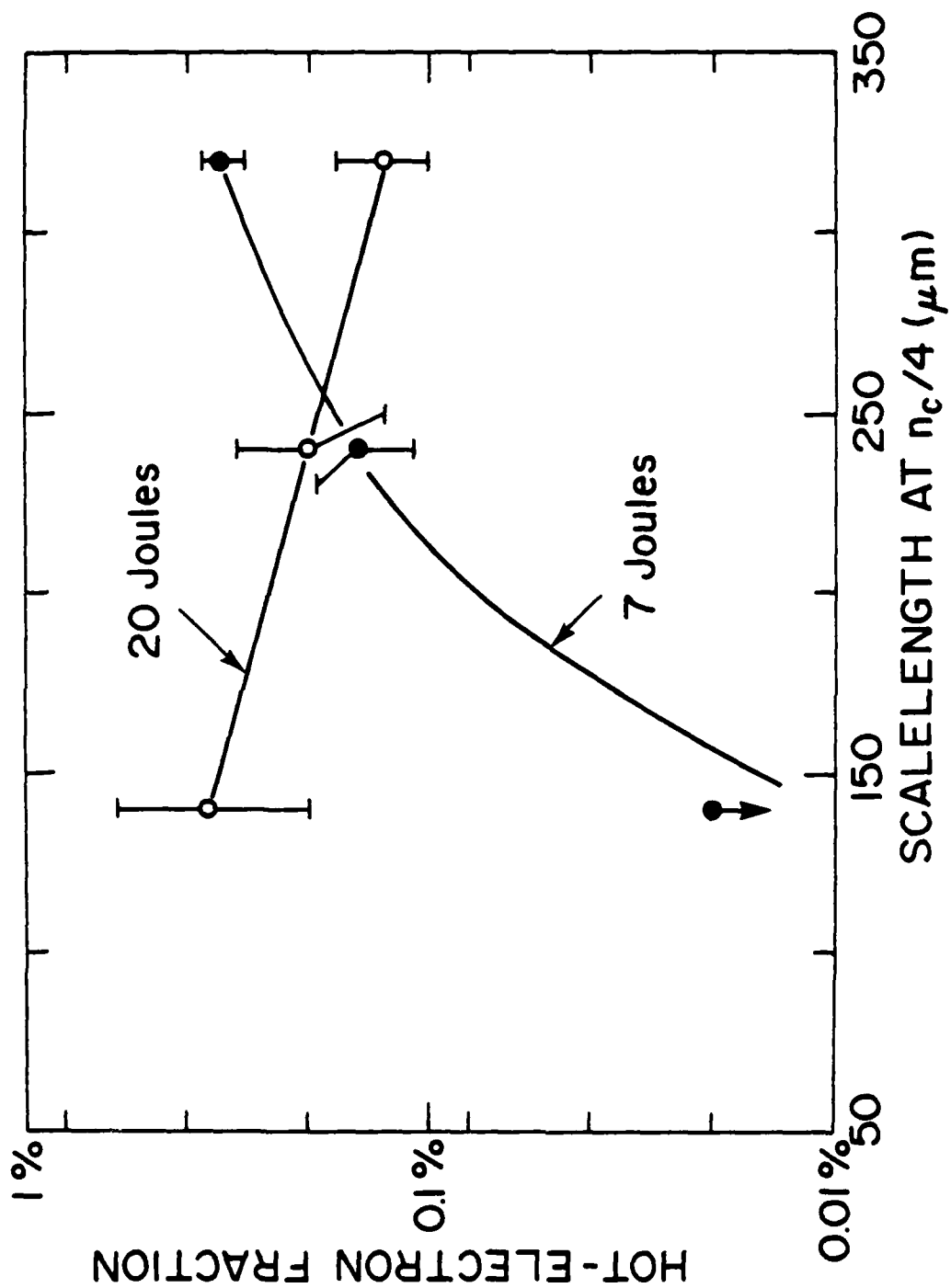
Figure 3

Hot-electron fractions for short-pulse energies of 7 J and 20 J as a function of the scalelength at $n_c/4$. The data point at 7 J and short scalelength is an upper limit.
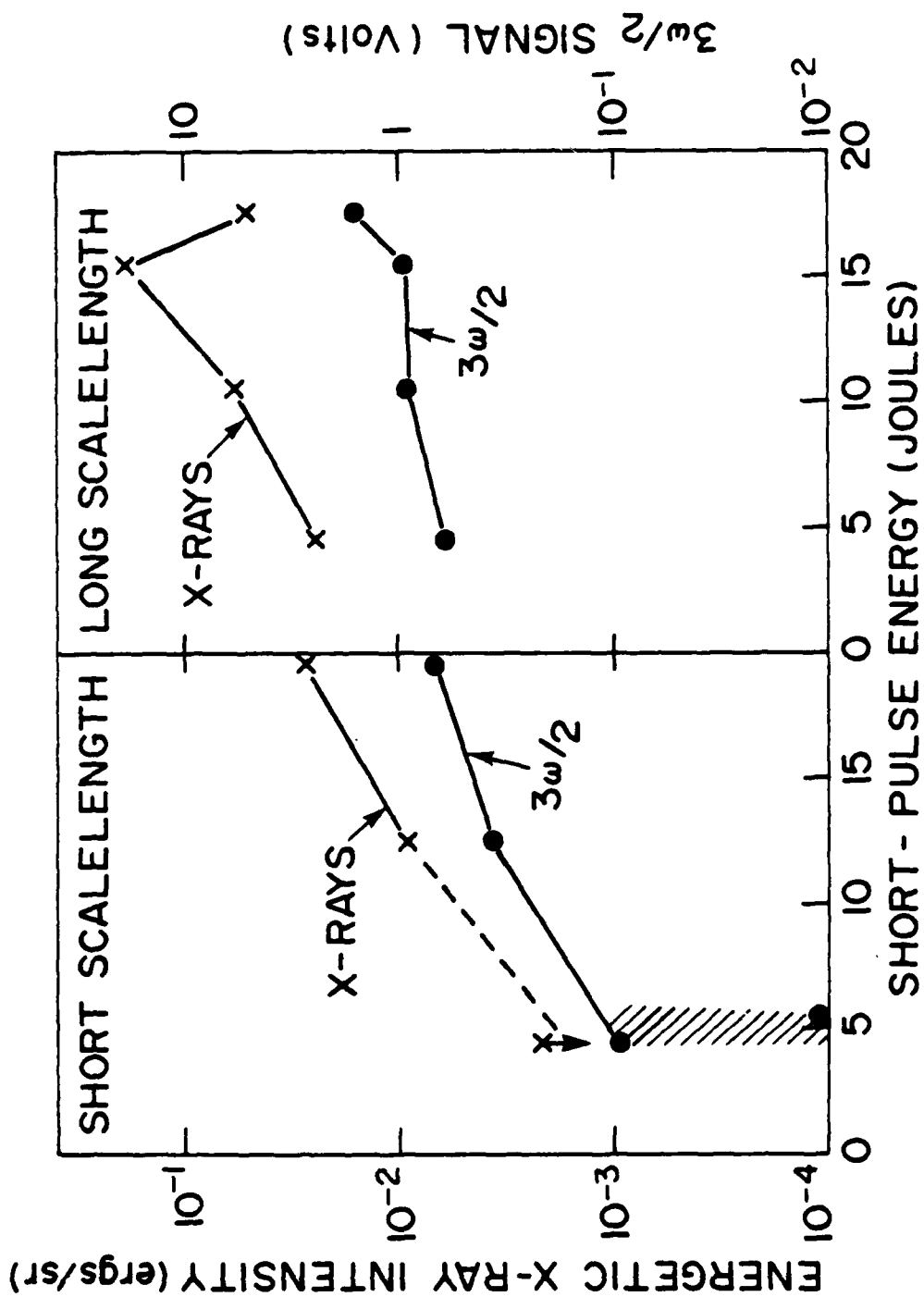
11

Figure 4

Intensities of energetic x-rays and 3w/2 emission (at 49° to the target normal) for short- and long-scalelength plasmas.

12

END

FILMED

3-85

DTIC